Carbon isotope evidence for the latitudinal distribution of air-sea gas exchange

Nir Y. Krakauer[1], James T. Randerson[2], François W. Primeau[2]

[1] *Division of Geological and Planetary Sciences, California Institute of Technology, Pasadena, CA 91125; niryk@caltech.edu*

[2] *Earth System Science, University of California, Irvine, CA 92697*

Introduction

The air-sea gas exchange rate determines the CO_2 flux into the ocean for a given pCO_2 disequilibrium at the sea surface. It is hard to measure directly, and how it varies by region remains unclear. A number of empirical formulas relating the air-sea exchange rate to windspeed are commonly used, but these span at least a factor of 2 at typical windspeeds (Fig. 1).

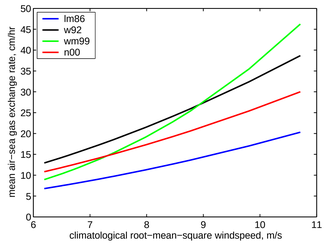

Figure 1. Some commonly-used published relationships for the increase in the air-sea gas exchange rate with windspeed (*1-4*).

Because windspeeds tend to be higher in the north and south than in the tropics (Fig. 2), all these formulas predict that the mean air-sea gas exchange is faster at high compared with low latitude oceans, although they would differ as to how much faster.

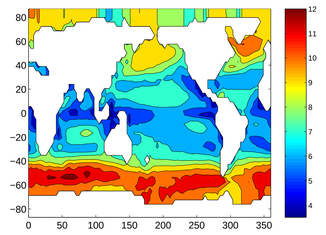

Figure 2. Root-mean-square winds (m/s) over the ocean for 1988-1992, based on satellite microwave scatter measurements (*5*).

We look at the effects on carbon-14, carbon-13 and total carbon fluxes of changing the global mean $\bar{k}$ and the windspeed dependence exponent n in a power law relationship of the air-sea gas exchange rate with windspeed:

$$k_w = (\frac{\bar{k}}{\bar{v}^n}) v^n (Sc/660)^{-0.5} \quad (1)$$

where

k_w = air-sea gas exchange rate (cm/hr)

$\bar{k}$ = global mean air-sea gas exchange rate (cm/hr)

v = windspeed at 10-m height (m/s)

n = exponent relating the gas exchange rate to windspeed

Sc = Schmidt number (water kinematic viscosity ÷ gas diffusivity).

Previous work with carbon-14 suggests 21±4 cm/hr for $\bar{k}$ (*6*). We vary the values of the parameters $\bar{k}$ and n about those used in the Ocean Carbon-Cycle Model Intercomparison Project (OCMIP) (*5*): $\bar{k}$ = 20.6 cm/hr and n = 2 (a quadratic dependence on windspeed). These reference values are marked with dotted lines in Figures 3, 6-8.

Modeling ocean bomb ^{14}C uptake

Model details

- Simulation for 1956-1997
- Transport fields from an ocean general circulation model
  - 3.75° * 3.75° horizontal resolution
  - z-coordinate, 29 vertical levels (50-300 m thick)
  - Gent-McWilliams parameterization for isopycnal mixing
  - KPP scheme for vertical mixing
  - Surface fluxes from a coupled atmosphere-ocean model run
  - Surface temperatures and salinities restored toward observed values
- Offline tracer advection using matrix exponentials (*7*)
- Boundary conditions largely follow OCMIP

Results

The modeled ocean bomb carbon-14 inventory is largely independent of the latitudinal distribution of air-sea gas exchange (as affected by the windspeed power-law exponent n), and thus is a good way of determining the global mean gas exchange rate $\bar{k}$ (Figure 3).

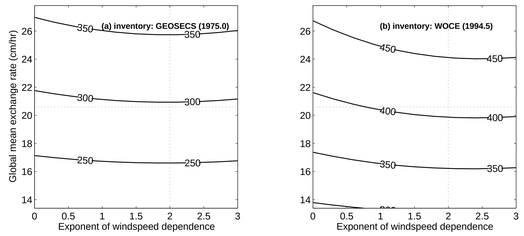

Figure 3. Modeled ocean bomb carbon-14 inventory in the mid-1970s and mid-1990s for different values of the air-sea gas exchange parameters $\bar{k}$ and n (Equation 1).

The *distribution* of the modeled bomb carbon-14 inventory is, however, affected by the windspeed exponent n adopted (Figure 4). A linear scaling of gas exchange with windspeed (n=1) fits the observed ocean bomb carbon-14 distribution better than a quadratic or cubic relationship (n=2 or 3), but part of this better match may be due to known problems with our ocean circulation model, such as too much mixing in the Southern Ocean.

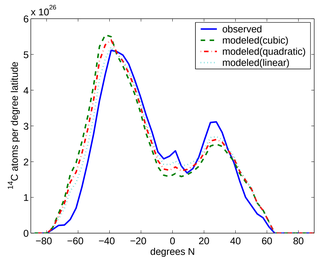

Figure 4. Modeled latitudinal distribution of bomb carbon-14 in the ocean for 1994 compared with gridded observations (*8*). The modeled distributions are for $\bar{k}$= 20.6 cm/hr and n = 3, 2, or 1 (in Equation 1).

The atmospheric $\Delta^{14}C$ gradient

Using regional Green's functions derived from an atmospheric transport model (*9*), we estimate the effect of carbon-14 isofluxes due to various processes on the latitudinal gradient in $\Delta^{14}C$ of atmospheric CO_2 (Figure 5a):

- Cosmogenic carbon-14 production – in upper atmosphere; north-south symmetric, effect on $\Delta^{14}C$ gradients at the surface depends on transport across the tropopause
- Biosphere respiration – releases old carbon that contains more bomb carbon-14 than the current atmospheric level
- Fossil fuel burning – releases very old carbon with no carbon-14
- Ocean exchange – large ocean uptake of carbon-14 in the Southern Ocean where the surface has low $\Delta^{14}C$; exchange in the tropics has little effect because sea surface $\Delta^{14}C$ is close to the atmospheric level.

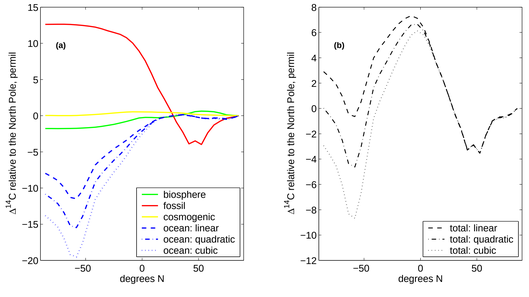

Figure 5. Modeled contributions to latitudinal variation in atmospheric $\Delta^{14}C$ by process for the mid-1990s. Ocean fluxes are based on observed sea-surface carbon-14 levels (*8*) and assume that air-sea gas exchange follows Equation 1 with $\bar{k}$ = 20.6 cm/hr and n = 3, 2, or 1.

The ocean exchange contribution varies depending on the assumed windspeed exponent n, and affects primarily the Southern Hemisphere gradient (Figure 5 and 6d). The size of ocean uptake would also be reflected in the contemporary rate of decline of atmospheric $\Delta^{14}C$ (Figure 6c) as well as in the near steady-state preindustrial $\Delta^{14}C$ levels and gradients (Figure 6ab).

Available measurements show relatively little depletion of $\Delta^{14}C$ over the Southern Ocean and a relatively low atmospheric $\Delta^{14}C$ decline rate, favoring a linear to quadratic increase of air-sea gas exchange with windspeed, i.e. n = 1-2 (Figure 6).

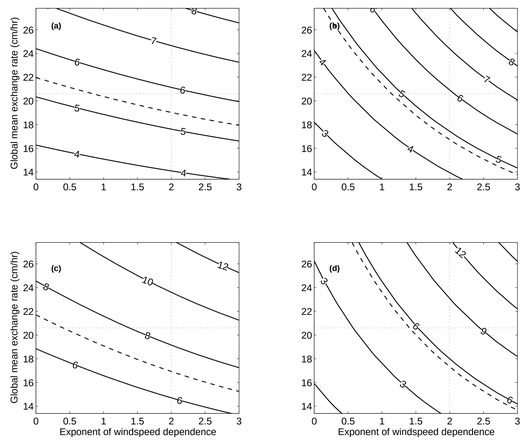

Figure 6. Effect of the air-sea gas exchange parameterization (Equation 1) on predicted total ocean carbon-14 uptake and on latitudinal gradients in atmospheric $\Delta^{14}C$. The dashed lines show the approximate uptake or latitudinal gradients inferred from observations for comparison. (a) Steady-state ocean carbon-14 uptake (in kg/year) assuming an estimated preindustrial sea-surface $\Delta^{14}C$ distribution (*8*) and mean atmospheric $\Delta^{14}C$ at 0 permil. For comparison, 5.4 kg/year would be needed to replace the decay of carbon-14 in ocean dissolved incorganic carbon. (b) Steady-state latitudinal atmospheric $\Delta^{14}C$ gradient (Britain – New Zealand, summer) in permil assuming an estimated preindustrial sea-surface $\Delta^{14}C$ distribution and mean atmospheric $\Delta^{14}C$ at 0 permil, calculated with an atmospheric transport model (*9*). For comparison, preindustrial tree-ring measurements reported by Hogg et al. (*10*) yield a difference of 4.8±1.6 permil. (c) Decline rate (in permil/year) of atmospheric $\Delta^{14}C$ around 1994, based on sea-surface $\Delta^{14}C$ interpolated from observations (*8*) and the estimated contributions of cosmogenic, land biosphere and fossil carbon fluxes. Observations yield a decline rate of 7.0±0.6 permil/year. (d) Latitudinal gradient in mean-annual atmospheric $\Delta^{14}C$ (Llano de Hato, Venezuela [9°N] – Macquarie Island [54°S]) around 1994, based on sea-surface $\Delta^{14}C$ interpolated from observations and the estimated contributions from other processes (Figure 5). Observations reported by Levin and Hesshaimer (*11*) yield a difference of 5.6±2.8 permil.

Air-sea ^{13}C and CO_2 exchange

Because the $\delta^{13}C$ of atmospheric CO_2 is dropping, there is an isotopic flux of carbon-13 out of the ocean. The $\delta^{13}C$ of the tropical oceans is higher than the equilibrium level, whereas the $\delta^{13}C$ of the high-latitude oceans is lower. Thus, the flux estimated based on observed sea surface $\delta^{13}C$ levels would vary substantially depending on the assumed windspeed power law exponent n (Figure 7). Independent observations of this flux are again consistent with n≤2.

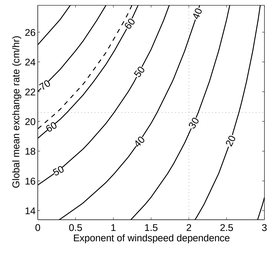

Figure 7. Predicted isoflux of carbon-13 into the ocean in PgC permil / year for 1994, based on WOCE sea-surface $\delta^{13}C$ measurements (*8*). The dashed contour shows the value of 62±32 PgC permil / year independently inferred from ocean interior observations (*12*).

We can combine measurements of the air-sea pCO_2 equilibrium in the mid-1990s with various relationships of the air-sea gas exchange rate with windspeed (Equation 1) to estimate the net uptake rate (Figure 8). The tropical oceans have high pCO_2 and release CO_2 into the atmosphere, whereas northern and southern oceans mostly have low pCO_2 and take up atmospheric CO_2. Higher values of n imply more exchange at high latitudes and less in the tropics, so that the oceans take up more CO_2 in all. Independent evidence for ocean CO_2 uptake is consistent with a value of 1-2 for n.

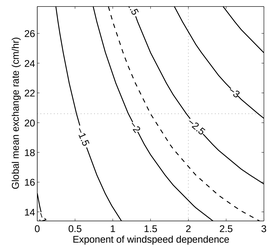

Figure 8. Predicted ocean anthropogenic CO_2 flux in PgC / year for 1995, based on the Takahashi et al. (*13*) pCO_2 climatology (corrected by 0.7 PgC / year for the assumed steady-state ocean outgassing that balances an inflow of continental carbon (*14*)). A dashed contour at −2.2 PgC / year shows the approximate anthropogenic ocean CO_2 uptake estimated using water ages inferred from ocean CFC measurements (2.0±0.4 PgC / year) (*15*) and based on atmospheric oxygen measurements (2.4±0.7 PgC / year) (*16*).

Conclusion

Measurements of carbon-14 in the ocean and atmosphere can constrain both the global mean air-sea gas exchange rate and its latitudinal distribution averaged over months to decades. Knowledge of the total air-sea carbon-13 and CO_2 fluxes can also be used to test proposed air-sea gas exchange distributions. Based on such data, it appears that the power law relationship with windspeed that best fits the distribution of the gas exchange rate has an exponent of between 1 and 2. Our approach supplements field measurements of gas exchange, which measure rates over relatively small areas and short periods.

References

1. P. S. Liss, L. Merlivat, in *The Role of Air-Sea Exchange in Geochemical Cycling* P. Buat-Ménard, Ed. (D. Reidel, Dordrecht, 1986) pp. 113-129.
2. R. Wanninkhof, *J. Geophys. Res.* 97, 7373-7382 (1992).
3. R. Wanninkhof, W. R. McGillis, *Geophys. Res. Lett.* 26, 1889-1892 (1999).
4. P. D. Nightingale *et al.*, *Global Biogeochem. Cycles* 14, 373-387 (2000).
5. J. C. Orr *et al.*, *Global Biogeochem. Cycles* 15, 43-60 (2001).
6. W. S. Broecker *et al.*, *J. Geophys. Res.* 91, 517-527 (1986).
7. F. Primeau, *J. Phys. Oceanogr.* 35, 545-564 (2005).
8. R. M. Key *et al.*, *Global Biogeochem. Cycles* 18, GB4031 (2004).
9. S. C. Olsen, J. T. Randerson, *J. Geophys. Res.* 109, D02301 (2004).
10. A. G. Hogg *et al.*, *Radiocarbon* 44, 633-640 (2002).
11. I. Levin, V. Hesshaimer, *Radiocarbon* 42, 69-80 (2000).
12. P. Quay, R. Sonnerup, T. Westby, J. Stutsman, A. McNichol, *Global Biogeochem. Cycles* 17, art. no. 1004 (2003).
13. T. Takahashi *et al.*, *Deep-Sea Res.* 49, 1601-1622 (2002).
14. O. Aumont *et al.*, *Global Biogeochem. Cycles* 15, 393-405 (2001).
15. B. I. McNeil, R. J. Matear, R. M. Key, J. L. Bullister, J. L. Sarmiento, *Science* 299, 235-239 (2003).
16. G. K. Plattner, F. Joos, T. F. Stocker, *Global Biogeochem. Cycles* 16, art. no. 1096 (2002).

Acknowledgements

We thank our funding sources: the Betty and Gordon Moore Foundation and the NASA Earth System Science Graduate Fellowship Program (NYK); NASA and NOAA (JTR).